Muon decay analysis with TWIST: recent progress

G.M. Marshall, for the TWIST Collaboration[1]

TRIUMF, 4004 Wesbrook Mall, Vancouver, BC, Canada V6T 2A3

Abstract. After a decade of design, construction, improvement, data-taking, simulation, and analysis, the TRIUMF Weak Interaction Symmetry Test (TWIST) muon decay parameter measurements are nearly complete. While the final results are yet to be unblinded, a preliminary estimate of the final precision is available. The goal of an order-of-magnitude improvement on pre-TWIST precisions for the ρ, δ, and $\mathscr{P}_\mu\xi$ decay parameters has essentially been achieved, making possible some tighter constraints on parameters of the left-right symmetric extension to the standard model as well as the fundamental coupling constants of the muon.

INTRODUCTION

The decay of polarized muons ($\mu \to e\nu\overline{\nu}$), where neither the electron polarization nor the accompanying neutrinos are observed, can be described by the differential rate as [1, 2, 3]

$$\frac{d^2\Gamma}{dx\, d\cos\theta} = \frac{1}{4} m_\mu W_{\mu e}^4 G_F^2 \sqrt{x^2 - x_0^2}\cdot \left\{\mathscr{F}_{IS}(x) + \mathscr{P}_\mu \cos\theta \cdot \mathscr{F}_{AS}(x)\right\}$$

where

$$W_{\mu e} = \frac{m_\mu^2 + m_e^2}{2m_\mu} \qquad \mathscr{P}_\mu = |\vec{\mathscr{P}}_\mu|$$
$$x = \frac{E_e}{W_{\mu e}} \qquad \cos\theta = \frac{\vec{\mathscr{P}}_\mu \cdot \vec{p}_e}{|\vec{\mathscr{P}}_\mu|\,|\vec{p}_e|}$$
$$x_0 = \frac{m_e}{W_{\mu e}}$$

The neutrino mass is neglected. Radiative corrections are not explicitly shown, but must be evaluated in the standard model to a precision compatible with experiment. The isotropic term $\mathscr{F}_{IS}(x)$ depends on the decay parameters ρ and η, while the asymmetric part $\mathscr{F}_{AS}(x)$ depends on δ and ξ. The TRIUMF Weak Interaction Symmetry Test (TWIST) has been constructed to determine the Michel parameter ρ as well as the parameters δ and $\mathscr{P}_\mu\xi$ with a precision approximately one order of magnitude higher than previous experiments, as a test of the standard model (SM).

Prior to 1990, the three decay parameters were known with uncertainties in the range of 7-16 parts per thousand. TWIST has reduced the uncertainties in the past few years (Fig. 1), to obtain [4, 5]

$$\begin{aligned}\rho &= 0.75014 \pm 0.00017(\text{stat}) \pm 0.00044(\text{syst}) \\ &\quad \pm 0.00011(\eta) \\ \delta &= 0.75067 \pm 0.00030(\text{stat}) \pm 0.00067(\text{syst}) \\ \mathscr{P}_\mu\xi &= 1.0003 \pm 0.0006(\text{stat}) \pm 0.0038(\text{syst})\end{aligned}$$

The decay parameters measured by TWIST contribute to a larger set derived from other observables, including one longitudinal and two transverse components of decay electron polarization and the cross section for inverse muon decay. An analysis can be made in terms of a generalized matrix element containing scalar, vector, and tensor interactions for muons and electrons of left and right chirality [6]. For a concise review, see [7]. A global analysis [4, 8] reveals consistency with the standard model, where the vector coupling for muons and electrons of left-handed chirality is the only non-zero term. The results from TWIST impact the upper limits of other terms, especially those for left-handed electrons and right-handed muons. The probability for right-handed muon couplings in muon decay has so far been reduced by a factor of two to less than 2.4×10^{-3} (90% confidence) by TWIST.

In left-right symmetric (LRS) extensions, there exists a heavier partner W' to the usual standard model W that

[1] `http://twist.triumf.ca/`: R. Bayes, Yu.I. Davydov, W. Faszer, M.C. Fujiwara, A. Grossheim, D.R. Gill, P. Gumplinger, A. Hillairet, R.S. Henderson, J. Hu, G.M. Marshall, R.E. Mischke, K. Olchanski, A. Olin, R. Openshaw, J.-M. Poutissou, R. Poutissou, G. Sheffer, B. Shin (TRIUMF), A. Gaponenko, R.P. MacDonald (University of Alberta), J.F. Bueno, M.D. Hasinoff (University of British Columbia), P. Depommier (Université de Montréal), E.W. Mathie, R. Tacik (University of Regina), V. Selivanov (Russian Research Center, Kurchatov Institute), C.A. Gagliardi, R.E. Tribble, (Texas A&M), D.D. Koetke, T.D.S. Stanislaus (Valparaiso University).

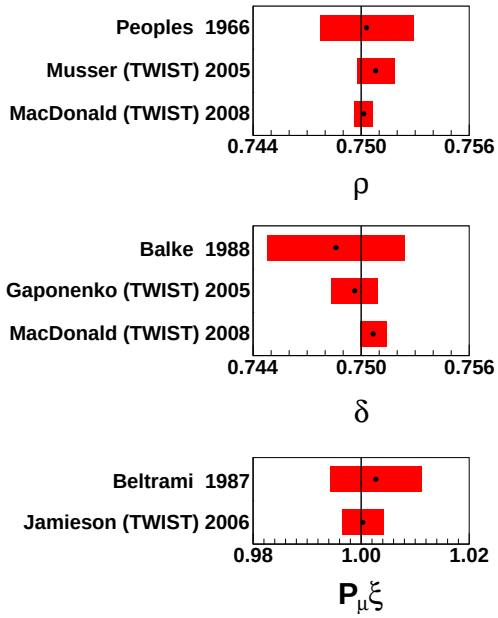

FIGURE 1. Summary of published values with uncertainties added quadratically for three muon decay parameters, including those prior to TWIST.

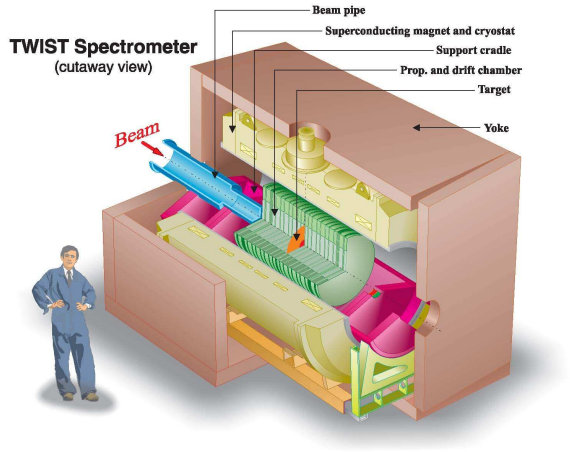

FIGURE 2. The TWIST spectrometer

mixes with angle ζ and couples dominantly to right-handed fermions. The effects of the W' could appear in muon decay. While other experiments are also sensitive to LRS interactions, muon decay is typically unaffected by assumptions of the model other than that the related right-handed neutrino is kinematically accessible.

EXPERIMENTAL DETAILS

The TWIST spectrometer is shown in Fig. 2. Highly polarized positive muons are selected from decays of stationary pions at the surface of a graphite production target. They are guided into the superconducting solenoidal field along its symmetry axis to enter a high precision, low mass stack of proportional and drift chambers [9]. The muons are ranged to stop predominantly in a metal foil at the center of the symmetric stack. Tracks from decay positrons in the uniform, precisely known 2 tesla field are defined by the low-mass drift chambers in a helium gas environment. Analysis yields two-dimensional distributions of positron angle and momentum (or energy) whose shape depends on the decay parameters. With a muon rate of order $2\text{–}5\times10^3$ s^{-1}, data sets of 10^9 events can be obtained in a few days. Approximately 3% of events pass event and track selection criteria as well as fiducial cuts on energy and angle. Much care is taken to test for and avoid the introduction of any bias. The fiducial cuts are symmetric for upstream and downstream decays, and are selected to maximize sensitivity to the decay parameters while reducing systematic uncertainties.

To determine the incoming muon beam characteristics (size, position, divergence, and correlations), another detector can be inserted to measure the beam before it enters the solenoid. This detector is a pair of time expansion chambers (TECs) recording the position and angle of each incident muon [10]. Since it causes multiple scattering and hence muon depolarization, it is typically removed for decay measurements, but the beam characteristics form an essential input to the simulation and analysis of decay data.

Decay positron reconstruction accounts for average energy loss, which depends on the helical track angle and thus the material traversed by the positron. It also allows for kinks in the track due to scattering at the drift chamber plane positions.

ANALYSIS PROCEDURES

The important principle of TWIST analysis is the comparison of energy-angle two-dimensional distributions of data to similar ones derived from a GEANT3 simulation. Both are subjected to essentially the same analysis, allowing bias and inefficiencies to be included in an equivalent way to reduce the dependence of the result on the specific procedure. This places great importance on the accuracy and detail of the simulation, requiring tests and verifications of several physical processes that determine, for example, muon stopping distribution, chamber response, time calibration, energy calibration, energy loss (bremsstrahlung and delta ray production), and de-

TABLE 1. Systematic uncertainties for ρ and δ from data obtained in 2004 [4]

Systematic uncertainties	$\rho(\times 10^{-4})$	$\delta(\times 10^{-4})$
Chamber response	2.9	5.2
Energy scale	2.9	4.1
Positron interactions	1.6	0.9
Resolution	0.2	0.3
Alignment and lengths	0.3	0.3
Beam intensity (ave)	0.1	0.2
Correlations with η	1.1	0.1
Theoretical radiative correction	0.3	0.1
Total	4.6	6.7

polarization. The simulation includes many detailed processes such as the following: incident muon beam descriptions are derived from TECs, and include correlations of muon track position and angle; muon polarization is tracked in the magnetic field to account for fringe field interactions; and, drift chamber ionization clusters are created with a statistical model that is consistent with chamber behaviour, including the electronic ionization detection threshold.

The decay parameters are obtained by a "blind" fit of the two-dimensional data distribution to that of a simulation base distribution, generated with hidden muon decay parameters, plus simulated distributions corresponding to the two-dimensional spectrum shape of first derivatives of the spectrum with respect to decay parameters (or combinations) ρ, ξ, and $\xi\,\delta$.

The fit of a base distribution to another one that includes derivative spectra also plays an imporant role in assessment of systematic uncertainties. Fits of data and/or simulation sets where a parameter or other input has been adjusted in one of them yields the effect of the adjustment in terms of the decay parameters. If the input is exaggerated, a statistically significant effect can be measured that can subsequently be scaled down to represent the potential systematic uncertainty on the decay parameter corresponding to the input parameter.

SYSTEMATIC UNCERTAINTIES: ρ, δ

The systematic uncertainties for our most precise published ρ and δ results arre shown in Table 1 [4]. Statistical uncertainties are considerably smaller. Three sources dominate: chamber response, energy scale, and positron interactions. Each has been improved substantially since that analysis, resulting in a much better precision for more recent data.

Chamber response refers to the conversion of drift chamber time information to spatial information used in helix fitting and evaluation of the momentum and angle

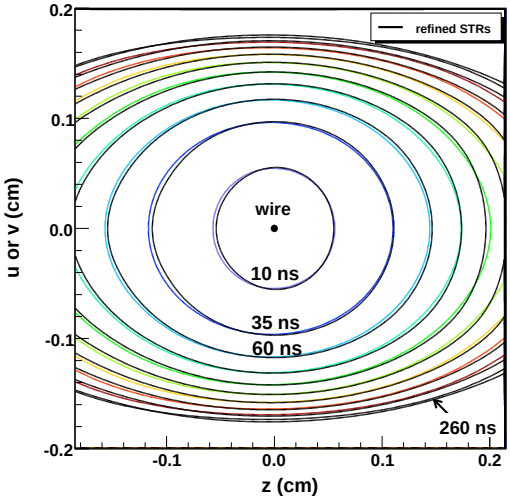

FIGURE 3. Drift time isochrones for data in a 4×4 mm^2 drift cell, before and after correction from track residual analysis. Corrections are specific to each detector plane. The z dimension is parallel to the spectrometer axis, while u and v are transverse.

of each track. Initially the space-time relations (STRs) were estimated from a simulation of the ionization and drift characteristics of the gas (dimethyl ether) using GARFIELD [11], but several effects were not accounted for. For example, small differential pressure variations caused cathode foil spacing changes, and temperature variations could affect STRs. To reduce these effects, substantial improvement in the control and monitoring of atmospheric effects was implemented.

Additionally, although the chambers were constructed to high precision and quality control standards, geometry variations did exist among the 44 DC planes. Moreover, the drift model was not perfect, and tracking biases existed that depended on STR consistency between data and simulation. To address all of these issues, a method was developed [12] by which the STRs were modified for each plane using positron decay track fit residuals to obtain self-consistent plane-dependent STRs. The tracking bias was reduced by applying the procedure also to simulations. Figure 3 shows data isochrones of the STRs before and after the procedure.

The maximum positron energy provides a calibration feature that is used to reduce the energy scale systematic. Since energy loss depends on the track angle primarily with a dependence on $1/\cos\theta$ due to the planar geometry of the detector, the energy region near the kinematic end point of 52.8 MeV/c is matched for data and simulation for small bins of $\cos\theta$. This procedure compensates for potential energy shift of up to ~ 10 keV/c due to small differences in mean stopping position of muons within the stopping target and also in magnetic field cal-

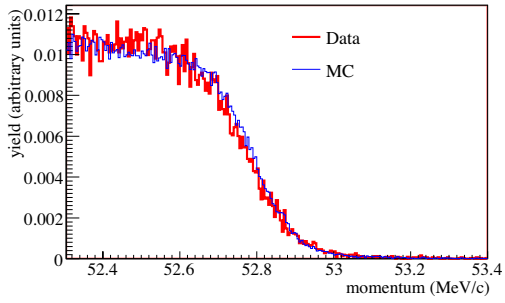

FIGURE 4. Comparison of data and simulation near the kinematic end point of the decay spectrum, for a narrow range of $\cos\theta$. The equivalent slopes prove that the resolution is simulated extremely well, while the small difference in position is corrected by an energy calibration procedure [4]

TABLE 2. Systematic uncertainties for $\mathscr{P}_\mu\xi$ from data obtained in 2004 [5]

Systematic uncertainties	$\mathscr{P}_\mu\xi\,(\times10^{-4})$
Depolarization in fringe field	34
Depolarization in stopping target	12
Chamber response	10
Spectrometer alignment	3
Positron interactions	3
Depolarization in production target	2
Energy calibration	2
Upstream-downstream efficiencies	2
Background muon contamination	2
Beam intensity variations	2
Correlations with η	1
Theoretical radiative correction	1
Total	38

ibration. The data-simulation relative energy calibration procedure has undergone improvements to become more robust to fitting conditions, while its sensitivity to data variations has been investigated. Due to inclusion of a realistic position-dependent resolution function and application of the previously mentioned self-consistent STR procedure, agreement of the detector resolution at the end point is remarkably good between data and simulation (Fig. 4).

Most other sources of systematic uncertainties for ρ and δ listed in Table 1 have been reduced as well, due to combinations of stricter control of experimental variables, more sensitive methods of evaluation, or improvements in analysis.

SYSTEMATIC UNCERTAINTIES: $\mathscr{P}_\mu\xi$

The asymmetry parameter ξ is also subject to uncertainties from the sources of the previous section, but they are overshadowed by other unique uncertainties related to depolarization (see Table 2). Because they appear only as a product $\mathscr{P}_\mu\xi$ in the differential decay rate, ξ and $\mathscr{P}_\mu$ cannot be determined separately.

The dominant contribution, from fringe field depolarization, depends on the accuracy with which the muon spin evolution can be simulated as the beam passes through significant radial field components at the solenoid entrance. The simulation in turn depends on two ingredients: an accurate field map, and precise knowledge of the position and direction of the muons in the beam. The longitudinal component of the magnetic field was measured throughout the volume occupied by the tracking detectors of the spectrometer, as well as within the region through which the muons entered. The beam measurement detectors (TECs) described above were placed in the mapped region. Individual muon tracks were measured with the TECs for the beam used in each data set, typically both before and after the data were taken. The distributions of the individual tracks in positions (x,y) and angles (θ_x,θ_y), including correlations, are used to initiate polarized muons in the simulation. The spin of each muon evolves according to the BMT (Bargmann-Michel-Telegdi) equation [13], closely following the momentum vector in the field in vacuum but deviating from it during scattering processes. In regions of significant radial field components, transverse momentum and spin components grow, thus reducing polarization along the field axis of the spectrometer. Simultations predict that the mean polarization $\mathscr{P}_\mu$ is reduced by 2×10^{-3} for a typical beam as it moves from the initial simulation point (location of TECs, field 0.1 tesla) to the stopping target (2.0 tesla), with the most rapid depolarization near the entrance to the spectrometer yoke (radial fields up to 0.017 tesla at 1 cm radius).

Alignment of the TECs used a combination of optical and collimated muon beam techniques. Alignment of the magnetic field map relied on optical and mechanical limits for translation, as well as positron decay helix axis angles for angular orientation. Consistency of the alignments in conjunction with the fringe field accuracy was tested by comparison of muon tracks in the TECs and in the upstream half of the decay spectrometer. Varying the TEC position and angle alignments quantified the dependence of depolarization to establish systematic alignment uncertainties for $\mathscr{P}_\mu\xi$. Special data sets taken with the beam mis-steered were more sensitive to fringe field variations. Differences in depolarization with respect to normal sets were compared to equivalent differences derived from corresponding simulations. Inconsistencies in these comparisons form the basis of the fringe field systematic estimate, and are still under scrutiny.

The second largest item of Table 2 is due to depolarization in the stopping target from muon spin relax-

ation (μ^+SR) as the spins interact with the target material. Though there are many potential mechanisms, it is believed that the dominant one is due to Korringa spin relaxation [14] from conduction electron spin contact interactions leading to an exponential time dependence. For TWIST, the mean polarization is measured at the time of decay, constrained to the range 1–9 μs after the muon stops. The exponential relaxation rates, λ, are determined from the time dependence of the relative upstream-downstream decay asymmetry to be $0.821 \pm 0.072\ \mathrm{ms}^{-1}$ and $1.250 \pm 0.081\ \mathrm{ms}^{-1}$, respectively, for the two stopping target materials, Ag and Al. The precision with which this relaxation is simulated is the source of both statistical and systematic uncertainties.

DECAY OF NEGATIVE MUONS IN ^{27}AL

The TWIST spectrometer was used for a period of several days to measure the decay electron distribution for negative muons stopped in the TWIST high purity aluminum target. The decay takes place from an atomic $\mu^- Al$ state that modifies the electron distribution. In particular, the decay-in-orbit allows a high energy component up to a value close to the 105.7 MeV muon rest energy limit that becomes important as a background in searches for muon-electron conversion. Because the response of the spectrometer is very well understood, and because a data set of reasonable statistics could be obtained in a short time, the radiative corrections became visible for the first time when compared to a lowest-order calculation [15]. This is shown in Fig. 5 [16].

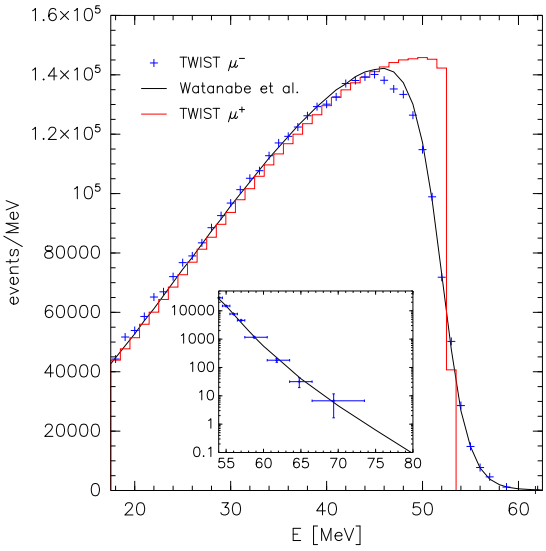

FIGURE 5. Energy distribution of electrons from μ^- decay in the TWIST Al target, compared with calculation [16]. The inset shows logarithmically the more energetic decay-in-orbit tail.

TABLE 3. Comparison of current and estimated final TWIST systematic uncertainties, along with improvement factors compared to pre-TWIST results.

	ρ	δ	$\mathscr{P}_\mu\xi$
Published [4, 5]			
Statistical($\times 10^{-4}$)	1.7	3.0	6.0
Systematic($\times 10^{-4}$)	4.4	6.7	38
Improvement factor *vs.* pre-TWIST	**×5**	**×5**	**×2**
Estimated, final			
Statistical($\times 10^{-4}$)	0.9	1.5	3.4
Systematic($\times 10^{-4}$)	2.8	3.0	12*
Improvement factor *vs.* pre-TWIST	**×9**	**×12**	**×7**

* Some challenges remain for final systematic uncertainty for $\mathscr{P}_\mu\xi$.

SUMMARY

Through a series of improvements to the apparatus, data-taking, and analysis procedures, a substantial improvement is expected for the final results of TWIST, compared to intermediate results and to prior experiments. Final checks of consistency and more precise estimates of systematic uncertainties are underway. Preliminary results are shown in Table 3, demonstrating that the goals of the experiment have been reached.

ACKNOWLEDGMENTS

This work was supported in part by the Natural Sciences and Engineering Research Council (NSERC) of Canada, the U.S. Department of Energy, the Russian Ministry of Science, and by TRIUMF. High performance computing resources for the analysis were provided by WestGrid (Canada).

REFERENCES

1. L. Michel, *Proc. Phys. Soc.* **A63**, 514 (1950).
2. C. Bouchiat, and L. Michel, *Phys. Rev.* **106**, 170 (1957).
3. A. Sirlin, *Phys. Rev.* **108**, 844 (1957).
4. TWIST Collaboration, R.P. MacDonald, et al., *Phys. Rev. D* **78**, 032010 (2008).
5. TWIST Collaboration, B. Jamieson, et al., *Phys. Rev. D* **74**, 072007 (2006).

6. W. Fetscher, H.-J. Gerber, and K. F. Johnson, *Phys. Lett.* **B173**, 102 (1986).
7. C. Amsler, and others (Particle Data Group), *Physics Letters* **B667** (2008).
8. C. Gagliardi, et al., *Phys. Rev. D* **72**, 073002 (2005).
9. R. L. Henderson, et al., *Nucl. Instr. and Meth. A* **548**, 306 (2005).
10. J. Hu, et al., *Nucl. Instr. and Meth. A* **566**, 563 (2006).
11. R. Veenhof, *GARFIELD, A Drift-Chamber Simulation Program, User's guide, ver 7.04*, CERN (2001).
12. A. Grossheim, et al. (in preparation).
13. V. Bargmann, L. Michel, and V. Telegdi, *Phys. Rev. Lett.* **2**, 435–436 (1959).
14. J. Korringa, *Physica* **16**, 601 (1950).
15. R. Watanabe, et al., *At. Data Nucl. Data Tables* **54**, 165 (1993).
16. TWIST Collaboration, A. Grossheim, et al., *Phys. Rev. D* **80**, 052012 (2009).